Ground-state energy and spin in disordered quantum dots

Kenji Hirose[1] and Ned S. Wingreen[2]

[1] *Fundamental Research Laboratories, NEC Corporation, 34 Miyukigaoka, Tsukuba, Ibaraki 305-8501, Japan*

[2] *NEC Research Institute, 4 Independence Way, Princeton, New Jersey 08540*

(February 1, 2008)

Abstract

We investigate the ground-state energy and spin of disordered quantum dots using spin-density-functional theory. Fluctuations of addition energies (Coulomb-blockade peak spacings) do not scale with average addition energy but remain proportional to level spacing. With increasing interaction strength, the even-odd alternation of addition energies disappears, and the probability of non-minimal spin increases, but never exceeds 50%. Within a two-orbital model, we show that the off-diagonal Coulomb matrix elements help stabilize a ground state of minimal spin.

73.61.-r, 71.15.Mb, 71.70.Ej, 75.75.+a

The control of spin in semiconductor nanostructures [1] is essential for a number of applications such as spintronics [2] and quantum bits [3], and for fundamental studies of the Kondo effect in quantum dots [4]. In clean quantum dots with circular symmetry, Hund's rule is observed – high-spin states (*i.e.* states of non-minimal spin) appear for partly filled shells of degenerate single-particle levels [5]. In disordered or chaotic quantum dots [6], high-spin states are suppressed by the rarity of degenerate or nearly degenerate levels. However, the observed absence of even-odd alternation of addition energies in quantum dots [7–10] is consistent with ground states of non-minimal spin. Recently, evidence for such high-spin states has been obtained from studies of the magnetic dispersion of Coulomb-blockade peaks [11,12]. A number of theoretical treatments have considered the conditions under which high-spin ground states might occur [13–20]. Many of these works [16,18,19] address the regime of large dimensionless conductance $g >> 1$ [21]; other works rely on the validity of the Hartree-Fock approximation [14,17]. Simulations on small lattice models indicate a significant fraction of $S = 1$ ground states [15], but we infer $g \sim 0.1 - 0.3$ in the simulations, compared to the experimental range $g > 1$ [7–10].

Density-functional theory enables *in silico* experiments on the ground-state spin of small, disordered quantum dots for which $g > 1$, over a wide range of interaction strengths. The results presented here challenge the view that high-spin states dominate in disordered dots for $r_s > 1$ [17]: even-odd alternation of addition energies disappears by $r_s = 1.25$, but the probability of a high-spin ground state never exceeds 50%. Using a two-orbital model, we show that off-diagonal Coulomb matrix elements help stabilize a ground states of minimum spin, as argued by Jacquod and Stone [20]. We also find that addition-energy fluctuations do not scale with the average addition energy, but remain proportional to the single-particle level spacing, consistent with our previous results for spin-polarized dots [25].

The ground-state energy and spin of disordered, two-dimensional quantum dots are obtained within spin-density-functional theory (SDFT). Specifically, we solve the following Kohn-Sham equations [22] numerically, and iterate until self-consistent solutions are obtained;

$$\left[-\frac{\hbar^2}{2m^*}\nabla^2+\frac{e^2}{\kappa}\int\frac{\rho(\mathbf{r}')}{|\mathbf{r}-\mathbf{r}'|}d\mathbf{r}'+\frac{\delta E_{\rm xc}[\rho,\zeta]}{\delta\rho^\sigma(\mathbf{r})}+\frac{1}{2}m^*\omega_0^2r^2+V_{\rm imp}(\mathbf{r})\right]\Psi_i^\sigma(\mathbf{r})=\epsilon_i^\sigma\Psi_i^\sigma(\mathbf{r}), \qquad (1)$$

where the density is $\rho(\mathbf{r})=\sum_\sigma\rho^\sigma(\mathbf{r})=\sum_\sigma\sum_i|\Psi_i^\sigma(\mathbf{r})|^2$, and the sum is taken over the N lowest-energy orbitals. Here σ denotes the spin index, $\zeta(\mathbf{r})$ is the local spin polarization, and $E_{\rm xc}[\rho,\zeta]$ is the exchange-correlation energy functional [23]. We use the effective mass for GaAs, $m^*=0.067m$, and a two-dimensional harmonic-oscillator confining potential with $\hbar\omega_0=3.0$meV. The dimensionless interaction strength is measured by $(e^2/\kappa\ell_0)/\hbar\omega_0$ or r_s [24] and is controlled by changing the dielectric κ, where $\kappa=12.9$ for GaAs.

We use the same parameters for the total impurity potential $V_{\rm imp}(\mathbf{r})=\sum_i(\gamma_i/2\pi\lambda^2)\exp\left(-|\mathbf{r}-\mathbf{r}_i|^2/2\lambda^2\right)$ as for a previous study of spin-polarized dots [25]. The density of individual impurities is $n_{\rm imp}=1.03\times10^{-3}\,{\rm nm}^{-2}$; each has a Gaussian potential profile, with strength γ_i distributed on $[-W/2,W/2]$ with $W=10\hbar^2/m^*$, and width $\lambda=\ell_0/(2\sqrt{2})$, where $\ell_0=\sqrt{\hbar/m^*\omega_0}\simeq19.5$nm is the quantum-confinement width of the parabolic potential. The resulting mean free path, $l=v_F\tau\simeq120$nm, is comparable to the dot diameter $L=120-160$nm, where L increases with interaction strength. Thus the dots are marginally in the ballistic regime and have a dimensionless conductance $g\sim2$ [21].

The density functional method is known to give accurate ground-state energies and spins for a *clean* dot [26]. Comparison with quantum-Monte-Carlo calculations [27] confirms that SDFT is valid for interaction strengths up to $(e^2/\kappa\ell_0)/\hbar\omega_0=6$ ($r_s\simeq8$) and up to 8 electrons. For disordered dots, we have confirmed the accuracy of the SDFT results by exact diagonalization studies of three electrons, over the range $0<(e^2/\kappa\ell_0)/\hbar\omega_0=2.86$ ($0<r_s<2.92$).

At low temperatures, electron hopping into a dot is suppressed except when the ground-state free energies for $N-1$ and N electrons are degenerate. This condition determines the position of the Nth conductance peak. The Nth peak spacing or addition energy is given by $\Delta(N)=E(N+1)-2E(N)+E(N-1)$, where the ground-state energy $E(N)$ is obtained from

$$E(N) = \sum_{i,\sigma} \epsilon_i^\sigma - \frac{e^2}{2\kappa} \int \frac{\rho(\mathbf{r})\rho(\mathbf{r}')}{|\mathbf{r}-\mathbf{r}'|} d\mathbf{r} d\mathbf{r}' - \sum_\sigma \int \rho^\sigma(\mathbf{r}) \frac{\delta E_{\rm xc}[\rho,\zeta]}{\delta \rho^\sigma(\mathbf{r})} d\mathbf{r} \; + \; E_{\rm xc}. \tag{2}$$

Figure 1 shows (a) the average addition energy $\langle\Delta\rangle$ and (b) its fluctuation $\delta\Delta \equiv \langle(\Delta - \langle\Delta\rangle)^2\rangle^{1/2}$, as functions of electron-electron interaction strength $(e^2/\kappa\ell_0)/\hbar\omega_0$ for $N = 10$ and $N = 11$. Dashed curves are for total spin fixed at its minimum, $S = 0$ or $1/2$. Solid curves are for unrestricted spin, *i.e.* the lowest energy $E(N)$ is found among all possible spin values. Also shown in (a) is the average *noninteracting* level spacing $\langle\Delta_0\rangle$ and in (b) its fluctuations $\langle\delta\Delta_0\rangle$, for dots of the same size as in the interacting case. In Fig. 1(a), there is an even-odd alternation in addition energies in the weak-interaction regime, $(e^2/\kappa\ell_0)/\hbar\omega_0 \leq 0.95$ ($r_s \leq 0.76$), which reflects the energy cost of adding every odd electron to a new orbital level. No alternation is observed in the regime of strong interactions ($r_s > 1$) where $\langle\Delta\rangle$ increases nearly linearly as a function of interaction.

In Fig. 1(b), the magnitudes of the addition-energy fluctuations for $N = 10$ and $N = 11$ merge around $r_s \sim 1.25$. The interacting fluctuations $\delta\Delta$ are always *smaller* than the fluctuations $\delta\Delta_0$ of the noninteracting level spacing, where the latter satisfy the random-matrix-theory relation for the Gaussian orthogonal ensemble [28] $\delta\Delta_0 \simeq \sqrt{4/\pi - 1}\langle\Delta_0\rangle \simeq 0.52\langle\Delta_0\rangle$. The interacting fluctuations are roughly $\delta\Delta \approx 0.28\langle\Delta_0\rangle$, and clearly do not scale with the average addition energy $\langle\Delta\rangle$. In fact, the interacting fluctuations are slightly smaller than those for the same number of interacting spin-*polarized* electrons in the same potential [25]. (In the spin-polarized case, the addition-energy fluctuations were shown to be dominated by the single-particle level-spacing fluctuations because of the effectiveness of screening in reducing the Coulomb fluctuations.)

Comparing Figs. 1 (a) and (b), one sees that in the range $r_s = 0.76 - 1.25$, the average addition energy is the same for $N = 10$ and $N = 11$, but the $N = 10$ distribution has a significantly larger width. For $r_s = 1.25$ and below, the shapes of the $N = 10$ and $N = 11$ distributions are qualitatively different [29] consistent with recent experiment observations for a high-electron-density GaAs quantum dot with $r_s = 0.72$ [11].

For the strong-interaction regime $r_s > 1$, fluctuations in addition energy are reduced

when the spin states are unrestricted. In the lower right inset, we show the distributions of $\Delta(N)$ for $N = 10$ (upper) and for $N = 11$ (lower) for interaction strength $(e^2/\kappa\ell_0)/\hbar\omega_0 = 1.91(r_s = 1.77)$, both for restricted and unrestricted spin. The distributions of Δ are roughly Gaussian, which agrees with experiments at $r_s > 1$ [7–10]. (For comparison, the Wigner-Dyson distribution [28] for the noninteracting case is shown in the upper left inset.) The distributions of Δ become narrower in the spin unrestricted case: the low-energy tail of the $N = 10$ distribution is reduced, while the high-energy tail is reduced for $N = 11$. We trace this behavior to the appearance of $S = 1$ ground states for 10 electrons (see below). Since $\Delta(N = 10) = E(11) - 2E(10) + E(9)$, the appearance of new, low values for $E(10)$ removes some of the *lowest* values of $\Delta(N = 10)$. Similarly, since $\Delta(N = 11) = E(12) - 2E(11) + E(10)$, new, low values of $E(10)$ remove some of the *highest* values of $\Delta(N = 11)$.

Figure 2(a) shows the probabilities of the different ground-state spins S versus electron-electron interaction strength. Solid curves are for $N = 10$ electrons (integer spin) and dashed curves are for $N = 11$ electrons (half-integer spin). With increasing interaction strength, the probabilities of ground states of $S = 1$, $3/2$, and 2 increase, while the probabilities of even higher spin states ($S = 5/2$, etc.) remain negligible. The probability of $S = 1$ for $N = 10$ is always higher than that of $S = 3/2$ for $N = 11$. The probability of an $S = 1$ ground state reaches a maximum around $(e^2/\kappa\ell_0)/\hbar\omega_0 \simeq 1.91(r_s \simeq 1.77)$, *and never exceeds 50%*. In the inset, we show the increase with interaction strength of the probability of spin blockade, *i.e.* subsequent ground states with $|\Delta S| > 1/2$, which leads to a suppressed Coulomb-blockade peak [30].

Diagonalization studies on small lattices also find a significant fraction of $S = 1$ ground states, with a smaller likelihood of $S = 3/2$ [15]. The onset of high-spin ground states occurs at smaller $r_s \sim 0.2$, and addition-energy fluctuations are larger, scaling as 10-20% of the average addition energy. We attribute these differences to weak screening in the lattic models due to the low dimensionless conductance of $g = 0.1 - 0.3$, compared to $g \sim 2$ in our dots.

Berkovits [15] has argued that high-spin ground states are favored not only by exchange energy (which favors spin alignment) but also by the enhanced Coulomb repulsion between two electrons in the same spatial orbital. Opposing these effects is the single-particle energy cost of promoting an electron to a new orbital. He observes that it is much more likely to find two orbitals close in energy, producing an $S = 1$ ground state, than to find three orbitals close in energy, as required for an $S = 3/2$ ground state.

These arguments are consistent with our SDFT results up to $r_s \simeq 1$, but do not account for the observed saturation of the probability of high-spin ground states at larger r_s. To understand this saturation, we consider the possible states of two electrons occupying two spin-degenerate orbitals near the Fermi energy. (The other electrons in the dot are assumed to pair up in lower-energy orbitals.) For this two-orbital model, there are three degenerate $S = 1$ states consisting of one electron in each of the two orbitals, and three nondegenerate $S = 0$ states.

To evaluate the energies of the competing $S = 0$ and $S = 1$ two-electron states, we use the basis of single-particle eigenstates $\phi^0_n(\mathbf{r})$ and $\phi^0_{n+1}(\mathbf{r})$ with energies ϵ_n and ϵ_{n+1} of non-interacting electrons. The various diagonal and off-diagonal Coulomb matrix elements are evaluated in the random-phase approximation (RPA) which accounts for the screening effect of the other electrons in the dot. The energy of the three degenerate $S = 1$ states is $\tilde{E}(S = 1) = \epsilon_n + \epsilon_{n+1} + \tilde{U}_{n,n+1} - \tilde{X}_{n,n+1}$, where $\tilde{U}_{n,n'} = e \int \tilde{\varphi}_{n,n}(\mathbf{r}) \rho^0_{n',n'}(\mathbf{r}) d\mathbf{r}$ is the screened Coulomb interaction between two electrons in orbitals n and n', and $\tilde{X}_{n,n'} = e \int \tilde{\varphi}_{n,n'}(\mathbf{r}) \rho^0_{n',n}(\mathbf{r}) d\mathbf{r}$ is the screened exchange interaction. Here, $\tilde{\varphi}_{n,n'}(\mathbf{r})$ is the screened potential due to an electron, which is evaluated in Fourier representation as $\tilde{\varphi}_{n,n'}(\mathbf{q}) = (2\pi e/\kappa|\mathbf{q}|)(\rho^0_{n,n'}(\mathbf{q})/\epsilon(\mathbf{q}))$, where $\rho^0_{n,n'}(\mathbf{r}) = \phi^0_n(\mathbf{r})\phi^0_{n'}(\mathbf{r})$. The dielectric function $\epsilon(\mathbf{q})$ is approximated as $\epsilon^{RPA}(\mathbf{q}) = 1 - v_q \chi(q)$ where $v_q = 2\pi/q$ and the susceptibility $\chi(q) = -(e^2/\kappa)(dn/d\mu)F(q/2k_F)$. The Lindhard polarizability for 2D is $F(x) = 1$ for $x \leq 1$ and $F(x) = 1 - \sqrt{1 - (1/x)^2}$ for $x \geq 1$.

The energy $\tilde{E}(S = 0)$ of the lowest $S = 0$ state is obtained by diagonalizing the following 3×3 matrix;

$$\tilde{H}_{S=0} = \begin{bmatrix} 2\epsilon_n + \tilde{U}_{n,n} & \sqrt{2}\tilde{U}_{n,n,n,n+1} & \tilde{X}_{n,n+1} \\ \sqrt{2}\tilde{U}_{n,n,n,n+1} & \epsilon_n + \epsilon_{n+1} + \tilde{U}_{n,n+1} + \tilde{X}_{n,n+1} & \sqrt{2}\tilde{U}_{n+1,n+1,n+1,n} \\ \tilde{X}_{n,n+1} & \sqrt{2}\tilde{U}_{n+1,n+1,n+1,n} & 2\epsilon_{n+1} + \tilde{U}_{n+1,n+1} \end{bmatrix} \quad (3)$$

where the off-diagonal Coulomb matrix elements are $\tilde{U}_{n,n,n,n'} = e\int \tilde{\varphi}_{n,n}(\mathbf{r})\rho^0_{n,n'}(\mathbf{r})d\mathbf{r}$. We find that the magnitudes of the $\tilde{U}_{n,n,n,n'}$ are comparable to the exchange energy $\tilde{X}_{n,n+1}$ [20]. It is seen in Fig. 2(b) that for the two-orbital model the average of $\Delta\tilde{E} \equiv \tilde{E}(S = 0) - \tilde{E}(S = 1)$ agrees reasonably well with our SDFT results for all strengths of interaction. In contrast, placing the two electrons in the lowest single-particle orbital $\phi^0_n(\mathbf{r})$, gives an energy $2\epsilon_n + \tilde{U}_{n,n}$ which is significantly larger than $\tilde{E}(S = 0)$ at large r_s. Even the Hartree-Fock (HF) approximation for (3), *i.e.* the best doubly-occupied single orbital, overestimates the energy of the lowest $S = 0$ state and fails to account for the saturation of the $S = 1$ probability at large r_s. It is evident that for the two-orbital model the off-diagonal Coulomb matrix elements help stabilize the $S = 0$ ground state by creating a low-energy hybridization of the three $S = 0$ basis states, as proposed by Jacquod and Stone [20].

We acknowledge fruitful discussions with B. Altshuler, R. Berkovits, D. Goldhaber-Gordon, B. Halperin, C. Marcus, M. Stopa, and F. Zhou.

REFERENCES

[1] L. L. Sohn, L. P. Kouwenhoven and G. Schön eds., *Mesoscopic Electron Transport*, (Kluwer, Dordrecht, 1997).

[2] G. A. Prinz, Science **282**, 1660 (1998).

[3] D. Loss and D. P. Divincenzo, Phys. Rev. **A57**, 120 (1998).

[4] D. Goldhaber-Gordon *et al.*, Nature **391**, 156 (1998); S. R. Cronenwett *et al.*, Science **281**, 540 (1998).

[5] S. Tarucha *et al.*, Phys. Rev. Lett. **77**, 3613 (1996).

[6] For reviews, see Y. Alhassid, Rev. Mod. Phys. **72**, 895 (2000), I. L. Aleiner, P. W. Brouwer, and L. I. Glazman, preprint cond-mat/0103008 v2.

[7] U. Sivan *et al.*, Phys. Rev. Lett **77**, 1123 (1996).

[8] F. Simmel *et al.* Europhys. Lett. **38**, 123 (1997).

[9] S. R. Patel *et al.*, Phys. Rev. Lett. **80**, 4522 (1998).

[10] F. Simmel *et al.* Phys. Rev. **B59** R10441 (1999).

[11] S. Lüscher *et al.*, Phys. Rev. Lett. **86**, 2118 (2001).

[12] J. A. Folk *et al.*, Physica Scripta **T90**, 26 (2001), (cond-mat/0010441) (2000).

[13] O. Prus *et al.*, Phys. Rev. **B54**, R14289 (1996).

[14] Y. M. Blanter, A. D. Mirlin, B. A. Muzykantskii, Phys. Rev. Lett. **78**, 2449 (1997).

[15] R. Berkovits, Phys. Rev. Lett. **81**, 2128 (1998).

[16] A. V. Andreev and A. Kamenev, Phys. Rev. Lett. **81**, 3199 (1998).

[17] P. W. Brouwer, Y. Oreg, and B. I. Halperin, Phys. Rev. **B60**, R13977 (1999).

[18] H. U. Baranger, D. Ullmo, and L. I. Glazman, Phys. Rev. **B61**, R2425 (2000).

[19] I. L. Kurland, I. L. Aleiner, and B. L. Altshuler, Phys. Rev. **B62**, 14886 (2000); I. L. Kurland, R. Berkovits, and B. L. Altshuler, Phys. Rev. Lett. **86**, 3380 (2001).

[20] P. Jacquod and A. D. Stone, Phys. Rev. Lett., **84**, 3938 (2000).

[21] The dimensionless conductance is given by $g = \hbar/(\tau_L \langle \Delta_0 \rangle)$ where the τ_L is the time an electron takes to cross the dot and $\langle \Delta_0 \rangle$ is the mean level spacing. For dots in the ballistic regime, such as those studied here, $g \sim k_F L/\pi$ where L is the linear size of the dot.

[22] W. Kohn and L. J. Sham, Phys. Rev. **140**, A1133 (1965).

[23] For the exchange-correlation energy, we use the local-density approximation $E_{\rm xc} = \int \rho(\mathbf{r})\, \epsilon_{\rm xc}[\rho(\mathbf{r}), \zeta(\mathbf{r})]\, d\mathbf{r}$, where $\epsilon_{\rm xc}[\rho(\mathbf{r}), \zeta(\mathbf{r})]$ is the parameterized form by Tanatar and Ceperley for the two-dimensional electron gas [B. Tanatar and D. M. Ceperley, Phys. Rev. **B39**, 5005 (1989)].

[24] The dimensionless interaction strength $r_s (= 1/\sqrt{\pi \rho_0} a_B^*)$ is the interparticle spacing in units of the effective Bohr radius a_B^*, where ρ_0 is the electron density at the center of the dot.

[25] K. Hirose, F. Zhou and N. S. Wingreen, Phys. Rev. **B63**, 075301 (2001).

[26] K. Hirose and N. S. Wingreen, Phys. Rev. **B59**, 4604 (1999).

[27] R. Egger *et al.*, Phys. Rev. Lett., **82**, 3320 (1999); F. Pederiva, C. J. Umrigar and E. Lipparini, Phys. Rev. **B62**, 8120 (2000).

[28] M. L. Mehta, *Random Matrices*, (Academic Press, Boston, 1991).

[29] K. Hirose and N. S. Wingreen, to be published.

[30] D. Weinmann, W. Häusler, and B. Kramer, Phys. Rev. Lett. **74**, 984 (1995).

Figure Captions

Figure 1: (a) Average addition energy $\langle\Delta\rangle$ and (b) fluctuation $\delta\Delta = \langle(\Delta - \langle\Delta\rangle)^2\rangle^{1/2}$, as functions of electron-electron interaction strength $(e^2/\kappa\ell_0)/\hbar\omega_0$ for $N = 10$ and $N = 11$. Solid curves are for unrestricted spin; dashed curves are for total spin fixed at $S = 0$ or $1/2$. For each data point, the disorder average is taken over more than 1000 different impurity configurations. The average noninteracting level spacing and its fluctuations are shown for the same size dots as in the interacting case. Lower right inset – Distribution of addition energies Δ for $N = 10$ (upper) and for $N = 11$ (lower) for interaction strength $(e^2/\kappa\ell_0)/\hbar\omega_0 = 1.94$. Upper left inset – Distribution of noninteracting addition energies (level spacings) for dots of the same size as in the lower inset.

Figure 2: (a) Probability of a spin S ground state as a function of electron-electron interaction strength $(e^2/\kappa\ell_0)/\hbar\omega_0$. Solid curves are for $N = 10$ electrons (integer spin) and dashed curves are for $N = 11$ electrons (half-integer spin). The circles give the probability of a spin $S = 1$ ground state for the full two-orbital model. Inset – Probability of spin blockade, *i.e.* subsequent ground states with $|\Delta S| > 1/2$. (b) Average total energy difference ΔE between states with $S = 0$ and $S = 1$ as a function of electron-electron interaction strength $(e^2/\kappa\ell_0)/\hbar\omega_0$. The solid curve shows the SDFT results. Also shown are results of the two-orbital model: exact (lowest dashed curve), Hartree-Fock (central dashed curve), doubly-occupied lowest orbital (highest dashed curve), with parameters evaluated for the $5th$ and $6th$ non-interacting orbitals. The apparent agreement between the HF result and SDFT at $r_s \sim 1$ is not meaningful – the HF result is only an approximation to the exact result (lowest dashed curve). Inset – Average level spacing and screened Coulomb interactions for two-orbital model.

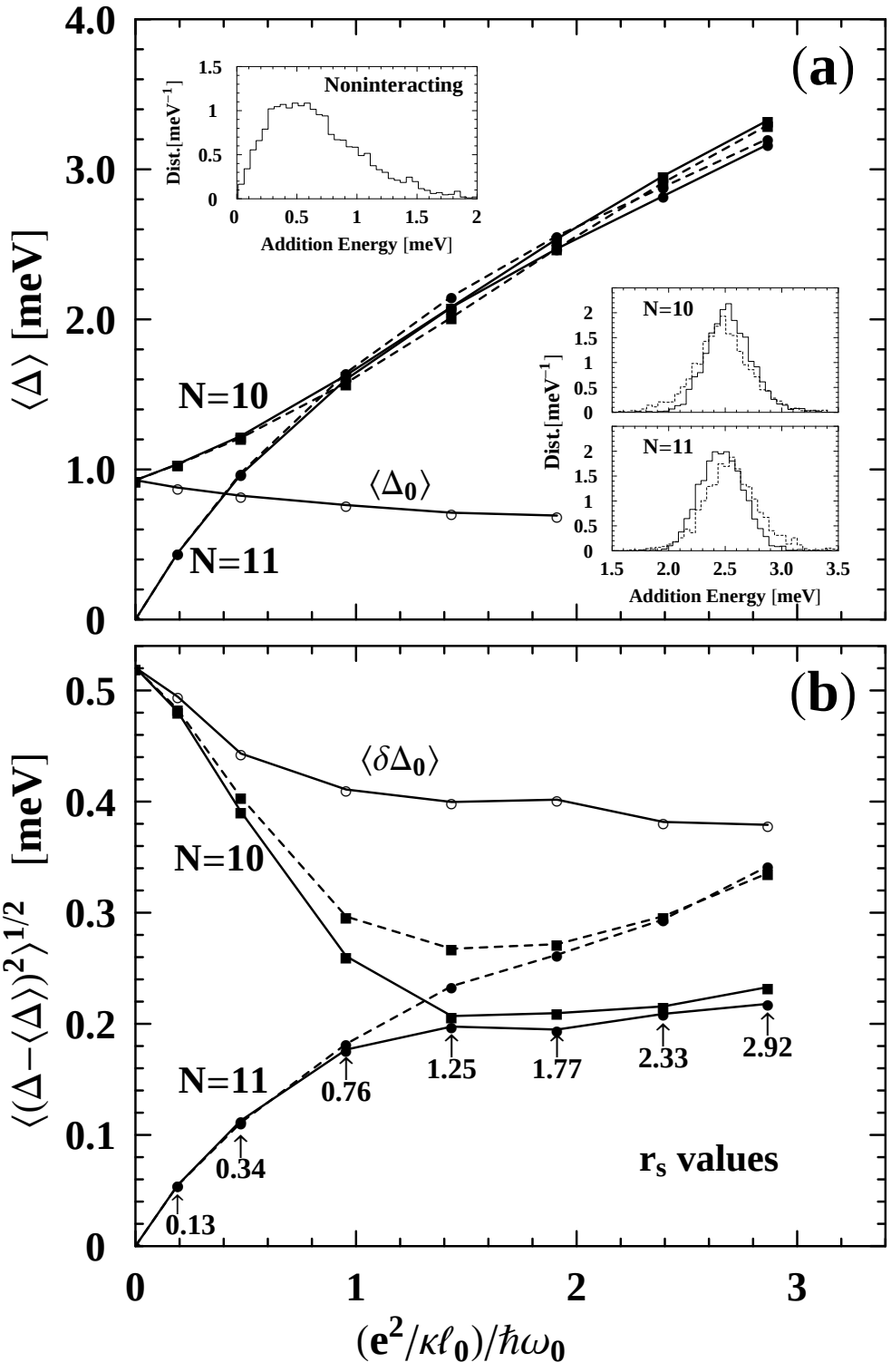
(a)
Noninteracting
Dist.[meV^{-1}]
Addition Energy [meV]
N=10
N=11
$\langle\Delta_0\rangle$
$\langle\Delta\rangle$ [meV]
(b)
$\langle\delta\Delta_0\rangle$
$\langle(\Delta-\langle\Delta\rangle)^2\rangle^{1/2}$ [meV]
0.13
0.34
0.76
1.25
1.77
2.33
2.92
r_s values
$(e^2/\kappa\ell_0)/\hbar\omega_0$

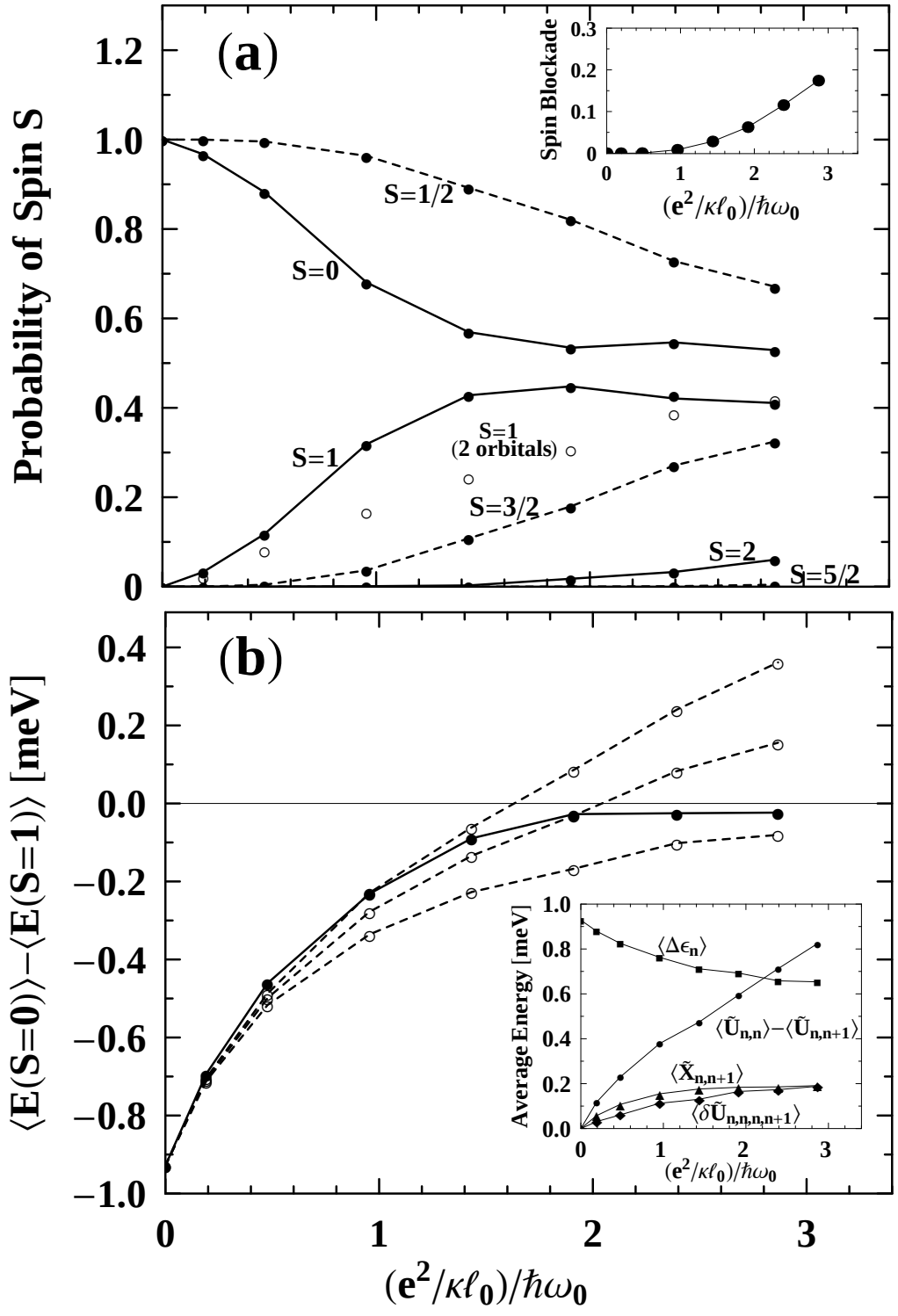
(a)
Probability of Spin S
S=1/2
S=0
S=1
S=1
(2 orbitals)
S=3/2
S=2
S=5/2
Spin Blockade
$(e^2/\kappa\ell_0)/\hbar\omega_0$
(b)
$\langle E(S=0)\rangle - \langle E(S=1)\rangle$ [meV]
Average Energy [meV]
$\langle\Delta\epsilon_n\rangle$
$\langle\tilde{U}_{n,n}\rangle - \langle\tilde{U}_{n,n+1}\rangle$
$\langle\tilde{X}_{n,n+1}\rangle$
$\langle\delta\tilde{U}_{n,n,n,n+1}\rangle$
$(e^2/\kappa\ell_0)/\hbar\omega_0$